Direct Observation of Electron Confinement in Epitaxial Graphene Nanoislands

Soo-hyon Phark,[†,*] Jérôme Borme,[‡] Augusto León Vanegas,[†] Marco Corbetta,[†] Dirk Sander,[†] and Jürgen Kirschner[†]

[†]Max-Planck-Institut für Mikrostrukturphysik, Weinberg 2, 06120 Halle, Germany and [‡]International Iberian Nanotechnology Laboratory, Avenida Mestre José Veiga, 4715-310 Braga, Portugal

The peculiar electronic properties of graphene (G) come from the π-band and result from the overlap of p_z orbitals on neighboring carbon atoms. A simple tight-binding (TB) model of G shows that energy dispersion of the π-band is described by $E = \pm v_F |\boldsymbol{p}|$, where the carrier momentum $\boldsymbol{p} = \hbar\boldsymbol{k}$ and the Fermi velocity $v_F \simeq 10^6$ m/s.[1−3] When carriers in G are confined, their properties depend on the confinement geometry. Previous studies showed how confinement of carriers in a G nanostructure affects the physical properties such as an electrical conductivity,[5−7] a size-dependent energy gap opening near the Dirac energy E_D,[8−10] and electronic edge states dependent on the edge atomic orientations.[11]

Surface inhomogeneities, such as defects or step edges, scatter the electrons and result in standing waves, so-called Friedel oscillation,[12] which provide crucial information, such as screening effect and electron−electron interaction, of an electron system. Experimental observation of such wave patterns in the metallic surface states has been done by scanning tunneling spectroscopy (STS)[4,13,14] since the technique measures the differential conductance (dI/dV) signal, which is proportional to the local density of states (LDOS) of the sample surface, with the spatial resolution down to the atomic scale.

The pseudospins and chirality of the G honeycomb structure are known to give rise to different scattering behaviors from those of two-dimensional (2D) Fermi electron gas,[15−17] for example, faster decay in the coherency of Friedel oscillation. Nevertheless, from the dimensional similarity, the same experimental approach with STS has been done and successfully obtained the G electronic properties such as energy dispersion

ABSTRACT One leading question for the application of graphene in nanoelectronics is how electronic properties depend on the size at the nanoscale. Direct observation of the quantized electronic states is central to conveying the relationship between electronic structures and local geometry. Scanning tunneling spectroscopy was used to measure differential conductance dI/dV patterns of nanometer-size graphene islands on an Ir(111) surface. Energy-resolved dI/dV maps clearly show a spatial modulation, indicating a modulated local density of states due to quantum confinement, which is unaffected by the edge configuration. We establish the energy dispersion relation with the quantized electron wave vector obtained from a Fourier analysis of dI/dV maps. The nanoislands preserve the Dirac Fermion properties with a reduced Fermi velocity.

KEYWORDS: scanning tunneling spectroscopy (STS) · quantum confinement · standing wave · epitaxial graphene · Dirac Fermion · electron dispersion relation

relations.[18−20] Recent theoretical calculations on the nanometer-size free-standing G flakes[21,22] predicted that quantization of wave vector k and energy E clearly depend on the size and symmetry of the flake geometry, as is true for the 2D Fermi electrons confined in a conventional metallic nanostructure. However, the shape and symmetry of the confined wave function are fairly different from those found in a conventional metallic nanostructure with the same geometry, due to the peculiar edge states.[23,24] Those results motivate the experimental studies on the confinement of Dirac electrons in a G nanostructure and the effects of the edge construction on it. However, there has been no report for the direct observation on the quantization of electronic states in an individual G nanostructure.

Here we show the STS measurements on regular and isogonal hexagonal G nanoislands on an Ir(111) surface. The dI/dV spectra and maps clearly show a spatial modulation, indicating a modulated local density of states, which is ascribed to quantum confinement. We find a quantized electron wave vector from a Fourier analysis of dI/dV maps.
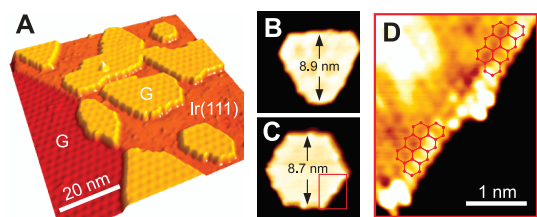
Figure 1. (A) STM image (70 × 70 nm^2) of G islands grown on Ir(111). (B,C) STM images of G nanoislands where electron confinement was investigated. See Figure 3. (D) Atomically resolved STM image in the edge region marked by the red rectangular box in C. G honeycomb lattice model is superimposed. Note that edges of the G nanoislands in our experiments showed zigzag-type arrangements of carbon atoms. Imaging parameters: $V_b = -0.05$ V, $I_{set} = 1$ nA (A,B); $V_b = -0.05$ V, $I_{set} = 2$ nA (C); $V_b = -0.03$ V, $I_{set} = 2$ nA (D).

Figure 2. (A) dI/dV curves measured from the center toward a corner of the island in Figure 1B. (B) dI/dV curves measured from the center toward a side of the island in Figure 1C. The inset in each plot shows the STM image with the positions where the dI/dV curves were taken. Measurement parameters: $V_{stab} = 0.5$ V, $I_{stab} = 1$ nA, $V_{mod} = 20$ mV (A,B); $V_b = -0.05$ V, $I_{set} = 1$ nA (insets of A and B).

The energy dispersion relation is described by the equation $E = E_D \pm \hbar v_F |\boldsymbol{k}|$ with $E_D = -0.09 \pm 0.02$ eV and $v_F = (6.0 \pm 0.4) \times 10^5$ m/s.

RESULTS AND DISCUSSION

Figure 1A shows G islands grown on an Ir(111) surface. Constant current scanning tunneling microscopy (STM) images reveal that all islands have a uniform apparent height of ~0.2 nm. The surface of the islands shows a pattern with a periodicity of 2.52 ± 0.03 nm, regardless of size and shape of the G islands (see Supporting Information I). This pattern is known as moiré structure. It is ascribed to a spatial pattern of the electronic properties due to the G—substrate interaction. The periodicity of the modulation arises from the superposition of the G and Ir(111) lattices.[25] The monatomic apparent height and the moiré patterns identify the formation of epitaxially ordered G islands. Figure 1B,C shows two G nanoislands on which we performed STS measurements. Figure 1D shows an atomic resolution image near an island edge showing the zigzag arrangement of the outermost carbon atoms.

Figure 2A,B shows dI/dV curves measured at different positions along the most symmetric directions of the islands shown in Figure 1B,C, respectively. As the measurement position moves from the center to the border, the curves clearly show a decrease in the amplitudes of the first peak at a bias voltage $V_b \approx -0.27$ V and an increase in the amplitudes of the second peak at $V_b \approx -0.41$ V. These V_b-dependent and spatially modulated dI/dV signals are ascribed to electron confinement, which induces a corresponding spatial modulation of LDOS.[26,27]

To provide clear evidence for electron confinement, we measure the maps of the dI/dV signal at different V_b. Figure 3A—E (Figure 3K—O) and Figure 3F—J (Figure 3P—T) show the dI/dV maps and their Fourier transform (FT) intensities of the patterns inside the islands of Figure 1B (Figure 1C). As we lower V_b from zero bias, the first modulation pattern (Figure 3A) is observed at $V_b = -0.27$ V. Here, the dI/dV signal shows
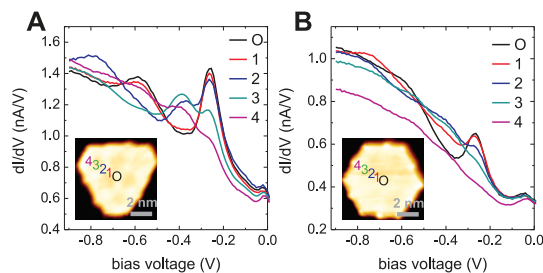
a maximum at the center and a monotonic decrease toward the border of the islands. For larger negative V_b, we identify four more distinct modulation patterns (Figure 3B—E). The patterns at lower V_b show an increasing number of modulations over the area of the island. The modulation can be understood as a standing wave pattern resulting from the interference of electron waves. Our findings suggest a decrease in the electron wavelength (increase in the electron wave vector) toward larger negative energy, as shown in Figure 4. For the island in Figure 1C, we also observed a similar tendency in both dI/dV and FT maps, as shown in Figure 3K—T. To compare the observed dI/dV maps to the LDOS of confined electrons, we employ the *multiple-scattering method*.[28,29] We extract the geometry from the STM images and use it for the calculation. The calculation reproduced very similar LDOS patterns with the same sequence of dI/dV modulation patterns (see Supporting Information II).

Interestingly, the energy intervals between any two neighboring patterns in Figure 3 are identical within our experimental accuracy, with an average separation of 0.16 eV. This marks a distinct difference between the energy dependence of dI/dV modulation patterns of G nanoislands as compared to those of metallic nanostructures.[13,27,30]

We obtain the wave vectors from the FT maps in Figure 3F—J (Figure 3P—T), which give rise to the modulation patterns of the dI/dV maps in Figure 3A—E (Figure 3K—O). The patterns of Figure 3 are selected to show the largest intensity of the respective $\boldsymbol{k}$-point. We observed that the intensity of a given $\boldsymbol{k}$-point of the FT map varies with energy. Also, the position does not vary continuously with energy but changes in a discrete manner. In 2D electron systems, the radial average of the FT map has been used to determine the in-plane wave vector $\boldsymbol{k}_\parallel$ of a standing wave pattern.[30−32] Under the same strategy, we take the average of the k for the sixfold symmetric pattern in each FT map as the magnitude of wave vector for each modulation pattern in Figure 3A—E (Figure 3K—O). The obtained values
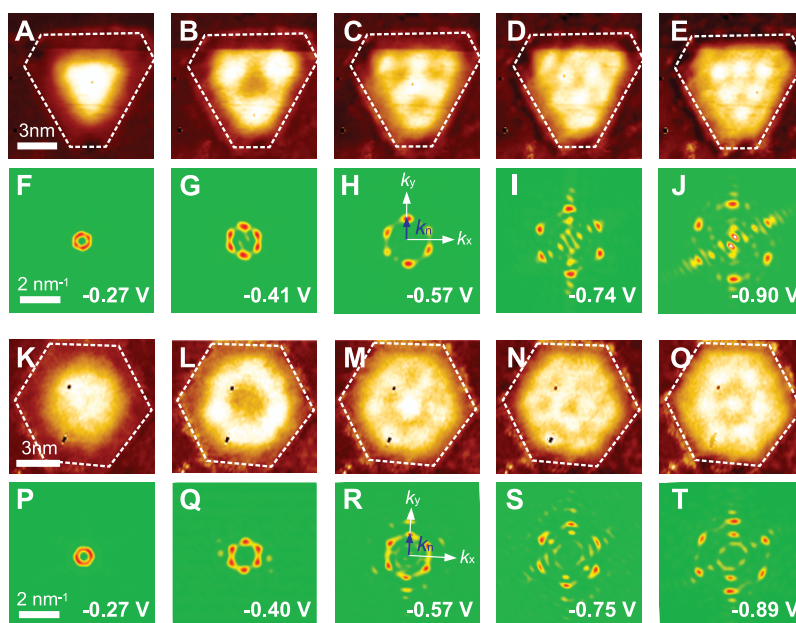
Figure 3. (A–J) dI/dV maps (A–E) and corresponding FT intensity maps (F–J) obtained from the island in Figure 1B. (K–T) dI/dV maps (K–O) and corresponding FT intensity maps (P–T) obtained from the island in Figure 1C. The bias voltage of each dI/dV map is denoted at the bottom-right side of the corresponding FT map. Dotted polygons in A–E and K–O indicate the boundaries of the nanoislands, as determined from the STM images in Figure 1B,C, respectively. Measurement parameters: V_{stab} = 0.5 V, I_{stab} = 1 nA, V_{mod} = 20 mV.
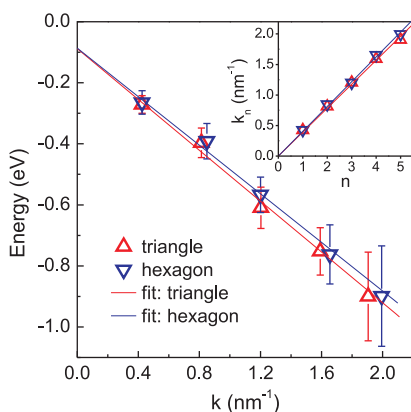

Figure 4. Dispersion relation $E(k)$ extracted from the dI/dV maps of the islands in Figure 1B (Figure 3A–E) and Figure 1C (Figure 3K–O), named "triangle" and "hexagon", respectively. E_D and v_F are extracted from the fit of the plots for each island with the equation $E = E_D - \hbar v_F k$. The inset shows the $k_n(n)$ plots extracted by applying 1D "particle-in-a-box" model to the wave vectors obtained from the FT maps in Figure 3. The slope of the fit gives the effective size of the confinement L_{eff}.

appear to be quantitatively very close to k for an intensity maximum of each FT map.

We obtain the dispersion relation from the extracted k and corresponding energy. Figure 4A shows a plot of (E,k) pairs obtained from the dI/dV modulation patterns shown in Figure 3. The discrete nature of k is apparent, which is a signature of the confinement. The plots clearly show a linear dependence of E on k, which is expected from the electronic dispersion relation predicted by the TB model of G.[1,3] Also, k increases monotonically as the electron energy gets more negative. This

implies that we observe quantized electron states of a filled π-band (hole states), which are identified by the dispersion relation $E = E_D - \hbar v_F |\boldsymbol{k}|$. A linear fit with the equation results in $E_D = -0.088 \pm 0.022$ eV (-0.086 ± 0.021 eV) and $v_F = (6.3 \pm 0.40) \times 10^5$ m/s ($(6.0 \pm 0.38) \times 10^5$ m/s) for the island in Figure 1B (Figure 1C).

The E_D offset of ~0.1 eV with respect to the Fermi energy (E_F) reflects a small substrate-induced charge doping in our nanoislands, similar to the infinitely large G/Ir(111) systems.[33–35] However, it is surprising that v_F values extracted from the plots in Figure 4A are smaller by 30–40% than the Fermi velocity of free-standing G (v_{F0}).

The G–substrate interaction is known to affect the graphene band structure. Angle-resolved photoemission spectroscopy (ARPES) has been employed to measure the band structure of G/Ir(111). Those experiments revealed the creation of minigaps[33,35] in the G π-band due to the moiré interaction and the hybridization of Ir surface states[36] with the G π-band at E_F. Nevertheless, the measured band structures showed the preservation of a linear π-band with the deviation of v_F from v_{F0} by only a few percent. Therefore, the G–substrate interaction itself appears to be not the only origin to explain the large reduction of v_F in our experiment.

We suggest another mechanism for the v_F reduction which could stem from the nanometer-size of the G islands in this study. In a TB model, v_F is described by $\hbar v_F = 3ta/2$, where a is the nearest carbon–carbon atomic distance and t is the nearest-neighbor hopping

amplitude through the π orbitals of carbon atoms. This expression with v_F extracted from our study gives a hopping amplitude $t \approx 1.7$ eV $\approx 0.6t_0$, where $t_0 = 2.8$ eV is the carbon−carbon hopping amplitude of freestanding G. It has been predicted that the modification in the hopping amplitude between carbon and impurity sites can locally reduce v_F due to the π orbital suppression at the defect sites.[37] Recent STM and STS measurements near the defects in G corroborated this view and reported a considerable reduction of v_F down to $\sim 0.3v_{F0}$.[19,20] Furthermore, these studies showed that the reduction of v_F extends over several nanometers around the defect sites. The edge atoms of G grown on Ir(111) are known to have a much stronger interaction with the substrate than those in the central region of the island.[38−40] The sharp decrease of the dI/dV signal near the island edge (see Supporting Information III) supports this view. This strongly suggests the suppression of the π-band in the near-edge regions. The edges of the islands, therefore, could act as extended lattice defects. Since the islands in this study have radii of 4−5 nm, one could expect a reduction of v_F over the whole area of the islands.

The noticeable difference between our work and the previous ARPES studies is the size of G. Thus, besides the G−substrate interaction, the small island sizes with the suppressed π-band near the edges provide one plausible scenario as a mechanism to induce the considerably small v_F in the nanometer-size G islands.

The survey of the effective size of the confinement L_{eff} would be an additional interesting aspect of the confinement phenomena in G as it is in the 2D Fermi electron confinement system. An effective way to obtain the confinement size along the symmetry axis of a threefold symmetric 2D structure by using a one-dimensional (1D) particle-in-a-box model has been introduced by Rodary et al.[13] We applied the same analogy to the G islands in Figure 3. We take the magnitude of the wave vector k_n along one of the symmetric direction, as indicated in Figure 3H,R, where n is the integer index determined from the sequence of dI/dV patterns shown in Figure 3A−E (Figure 3K−O).

The inset of Figure 4 shows the plots of k_n as a function of n. Each data set is fitted well by a linear function $k_n = n\pi/L_{eff}$ intersecting the origin. The slope of the $k_n(n)$ relation gives $L_{eff} = 8.4$ nm (8.0 nm) for the island in Figure 1B (Figure 1C), which is approximately 0.5 (0.7) nm smaller than the geometric size as indicated in Figure 1B (Figure 1C). The above-mentioned strong interaction of the edge carbon atom is expected to deplete the electronic DOS near the island edge. It is plausible that such an effect extends to 2−3 unit cells (0.5−0.7 nm) from the island edge (see Supporting Information III). This may indicate that the sharp transition of the electronic properties near the island edge serves as the potential barrier for confinement, leading to a smaller L_{eff} as compared to the geometric size.

CONCLUSIONS

In conclusion, we perform STM and STS measurements of G islands on Ir(111). We observe a pronounced spatial modulation of the differential conductance dI/dV in nanosized monolayer G. We ascribe this to a spatial modulation of the LDOS, which is induced by electron confinement. The quantitative analysis of the modulation patterns using FT maps gives the electron dispersion, which is well described by Dirac Fermion dispersion $E = E_D - \hbar v_F k$ with $E_D \approx -0.09$ eV and $v_F \approx 6 \times 10^5$ m/s. The π-band modification by the G-substrate interaction itself appears to be not the only origin to explain the large reduction of v_F in the nanoislands. The finite size effect, where the edge scattering contributes, may contribute as an other possible mechanism. Additionally, to derive the confinement size L_{eff}, we apply the 1D partical-in-a-box model to the symmetry axis of the islands. The extracted L_{eff} is smaller by 2−3 G unit cells than the geometric size. This difference may stem from the strong carbon−substrate interaction at the island edges, giving rise to the depletion of G DOS in the near-edge regions. Our results show clear electron confinement effects in G nanostructures unperturbed by the zigzag edge configuration. G nanoislands on Ir(111) provide a new good platform to understand the pure quantum confinement effect in G.

METHODS

The experiments are performed in an ultrahigh vacuum (UHV) chamber equipped with a scanning tunneling microscope (STM) operating at 8 K and a chamber for sample preparation. The STM chamber is equipped with ^{4}He bath cryostat operating at a base pressure (P_b) of 2×10^{-11} mbar. The preparation chamber is connected to the STM chamber by a gate valve and operates at $P_b = 2 \times 10^{-10}$ mbar. The Ir(111) single crystal (MaTeck GmbH) was Ar$^+$-sputtered at room temperature (RT) (1 keV, 0.75 μA, 15 min) and subsequently heated 10 times to 1200 K in an O$_2$ pressure of 1×10^{-8} mbar. Finally, it was annealed at 1370 K at $P_b = 2 \times 10^{-10}$ mbar. In order to grow monolayer graphene, the cleaned Ir(111) surface was exposed to C$_2$H$_4$ at RT and a pressure of 2×10^{-9} mbar for 2 min and subsequently heated to 1320 K for 2 min under the same partial pressure of C$_2$H$_4$. The sample was then transferred to the STM chamber. STM images show that $\sim$60% of the substrate surface is covered by G islands. Their sizes ranges from 6 to 50 nm in diameter. We perform STM and STS measurement on the G islands at 8 K and 2×10^{-11} mbar. The STM images are obtained in constant-current mode. For STS, we employed a standard lock-in technique with modulation frequency $\nu = 4$ kHz and root-mean-squared amplitude of 20 mV. Before each STS measurement, the tunneling condition was stabilized at $V_{stab} = 0.5$ V, $I_{stab} = 1$ nA.

Supporting Information Available: Supporting Information material is composed of three sections, sequentially labeled I, II, and III. The first section shows typical properties of the G/Ir(111) sample. The second section shows the calculated LDOS patterns by multiple-scattering method. The third section shows the STS curves at an edge region of a G island. This material is available free of charge *via* the Internet at http://pubs.acs.org.

REFERENCES AND NOTES

1. Wallace, P. R. The Band Theory of Graphite. *Phys. Rev.* **1947**, *71*, 622.
2. Geim, A. K.; Novoselov, K. S. The Rise of Graphene. *Nat. Mater.* **2007**, *6*, 183–191.
3. Castro Neto, A. H.; Guinea, F.; Peres, N. M. R.; Novoselov, K. S.; Geim, A. K. The Electronic Properties of Graphene. *Rev. Mod. Phys.* **2009**, *81*, 109–162.
4. Crommie, M. F.; Lutz, C. P.; Eigler, D. M. Imaging Standing Waves in a Two-Dimensional Electron Gas. *Nature* **1993**, *363*, 524–527.
5. Berger, C.; Song, Z.; Li, X.; Wu, X.; Brown, N.; Naud, C.; Mayou, D.; Li, T.; Hass, J.; Marchenkov, A. N.; *et al.* Electronic Confinement and Coherence in Patterned Epitaxial Graphene. *Science* **2006**, *312*, 1191–1196.
6. Han, M. Y.; Ozyilmaz, B.; Zhang, Y. B.; Kim, P. Energy Band-Gap Engineering of Graphene Nanoribbons. *Phys. Rev. Lett.* **2007**, *98*, 206805.
7. Li, X. L.; Wang, X. R.; Zhang, L.; Lee, S. W.; Dai, H. J. Chemically Derived, Ultrasmooth Graphene Nanoribbon Semiconductors. *Science* **2008**, *319*, 1229–1232.
8. Tapasztó, L.; Dobrik, G.; Lambin, P.; Biró, L. P. Tailoring the Atomic Structure of Graphene Nanoribbons by Scanning Tunneling Microscope Lithography. *Nat. Nanotechnol.* **2008**, *3*, 397–401.
9. Ritter, K. A.; Lyding, J. W. The Influence of Edge Structure on the Electronic Properties of Graphene Quantum Dots and Nanoribbons. *Nat. Mater.* **2009**, *8*, 235–242.
10. Lu, J.; Yeo, P. S. E.; Gan, C. K.; Wu, P.; Loh, K. P. Transforming C_{60} Molecules into Graphene Quantum Dots. *Nat. Nanotechnol.* **2011**, *6*, 247–252.
11. Tao, C.; Jiao, L.; Yazyev, O. V.; Chen, Y.-Z.; Feng, J.; Zhang, X.; Capaz, R. B.; Tour, J. M.; Zettl, A.; Louie, S. G.; *et al.* Spatially Resolving Edge States of Chiral Graphene Nanoribbons. *Nat. Phys.* **2011**, *7*, 616–620.
12. Friedel, J. Metallic Alloys. *Nuevo Cimento* **1958**, *7*, 287.
13. Rodary, G.; Sander, D.; Liu, H.; Zhao, L.; Niebergall, L.; Stepanyuk, V. S.; Bruno, P.; Kirschner, J. Quantization of the Electron Wave Vector in Nanostructures: Counting *k*-States. *Phys. Rev. B* **2007**, *75*, 233412.
14. Oka, H.; Ignatiev, P. A.; Wedekind, S.; Rodary, G.; Niebergall, L.; Stepanyuk, V. S.; Sander, D.; Kirschner, J. Spin-Dependent Quantum Interference within a Single Magnetic Nanostructure. *Science* **2010**, *327*, 843–846.
15. Cheianov, V. V. Impurity Scattering, Friedel Oscillation and RKKY Interaction in Graphene. *Eur. Phys. J. Special Topics* **2007**, *148*, 55–61.
16. Yang, H.; Mayne, A. J.; Boucherit, M.; Comtet, G.; Dujardin, G.; Kuk, Y. Quantum Interference Channeling at Graphene Edges. *Nano Lett.* **2010**, *10*, 943–947.
17. Simon, L.; Bena, C.; Vonau, F.; Cranney, M.; Aubel, D. Fourier Transform Scanning Tunneling Spectroscopy: The Possibility To Obtain Constant Energy Maps and Band Dispersion Using a Local Measurement; arXiv:1107.3648v1, **2011**.
18. Rutter, G. M.; Crain, J. N.; Guisinger, N. P.; Li, T.; First, P. N.; Stroscio, J. A. Scattering and Interference in Epitaxial Graphene. *Science* **2007**, *317*, 219–222.
19. Tapasztó, L.; Dobrik, G.; Nemes-Incze, P.; Vertesy, G.; Lambin, Ph.; Biró, L. P. Tuning the Electronic Structure of Graphene by Ion Irradiation. *Phys. Rev. B* **2008**, *78*, 233407.
20. Simon, L.; Bena, C.; Vonau, F.; Aubel, D.; Nasrallah, H.; Habar, M.; Peruchetti, J. C. Symmetry of Standing Waves Generated by a Point Defect in Epitaxial Graphene. *Eur. Phys. J. B* **2009**, *69*, 351–355.
21. Heiskanen, H. P.; Manninen, M.; Akola, J. Electronic Structure of Triangular, Hexagonal and Round Graphene Flakes near the Fermi Level. *New J. Phys.* **2008**, *10*, 103015.
22. Rozhkov, A. V.; Nori, F. Exact Wave Functions for an Electron on a Graphene Triangular Quantum Dot. *Phys. Rev. B* **2010**, *81*, 155401.
23. Nakada, K.; Fujita, M.; Dresselhaus, G.; Dresselhaus, M. S. Edge State in Graphene Ribbons: Nanometer Size Effect and Edge Shape Dependence. *Phys. Rev. B* **1996**, *54*, 17954.
24. Son, Y.-W.; Cohen, M. L.; Louie, S. G. Energy Gaps in Graphene Nanoribbons. *Phys. Rev. Lett.* **2006**, *97*, 216803.
25. N'Diaye, A. T.; Coraux, J.; Plasa, T. N.; Busse, C.; Michely, T. Structure of Epitaxial Graphene on Ir(111). *New J. Phys.* **2008**, *10*, 043033.
26. Li, J.; Schneider, W.-D.; Crampin, S.; Berndt, R. Tunneling Spectroscopy of Surface State Scattering and Confinement. *Surf. Sci.* **1999**, *422*, 95–106.
27. Kliewer, J.; Berndt, R.; Crampin, S. Scanning Tunneling Spectroscopy of Electron Resonators. *New J. Phys.* **2001**, *3*, 22.
28. Heller, E. J.; Crommie, M. F.; Lutz, C. P.; Eigler, D. M. Scattering and Absorption of Surface Electron Waves in Quantum Corrals. *Nature* **1994**, *369*, 464–466.
29. Crommie, M. F.; Lutz, C. P.; Eigler, D. M.; Heller, E. J. Quantum Corrals. *Physica D* **1995**, *83*, 98–108.
30. Diekhöner, L.; Schneider, M. A.; Baranov, A. N.; Stepanyuk, V. S.; Bruno, P.; Kern, K. Surface States of Cobalt Nanoislands on Cu(111). *Phys. Rev. Lett.* **2003**, *90*, 236801.
31. Petersen, L.; Sprunger, P. T.; Hofmann, Ph.; Lægsgaard, E.; Briner, B. G.; Doering, M.; Rust, H.-P.; Bradshaw, A. M.; Besenbacher, F.; Plummer, E. W. Direct Imaging of the Two-Dimensional Fermi Contour: Fourier-Transform STM. *Phys. Rev. B* **1998**, *57*, R6858–R6861.
32. Schouteden, K.; Lijnen, E.; Janssens, E.; Ceulemans, A; Chibotaru, L; Lievens, P.; Van Haesendonck, C. Confinement of Surface State Electrons in Self-Organized Co Islands on Au(111). *New J. Phys.* **2008**, *10*, 043016.
33. Pletikosić, I.; Kralj, M.; Pervan, P.; Brako, R.; Coraux, J.; N'Diaye, A. T.; Busse, C.; Michely, T. Dirac Cones and Minigaps for Graphene on Ir(111). *Phys. Rev. Lett.* **2009**, *102*, 056806.
34. Rusponi, S.; Papagno, M.; Moras, P.; Vlaic, S.; Etzkorn, M.; Sheverdyaeva, P. M.; Pacilé, D.; Brune, H.; Carbone, C. Highly Anisotropic Dirac Cones in Epitaxial Graphene Modulated by an Island Superlattice. *Phys. Rev. Lett.* **2010**, *105*, 246803.
35. Kralj, M.; Pletikosić, I.; Petrović, M.; Pervan, P.; Milun, M.; N'Diaye, A. T.; Busse, C.; Michely, T.; Fujii, J.; Vobornik, I. Graphene on Ir(111) Characterized by Angle-Resolved Photoemission. *Phys. Rev. B* **2011**, *84*, 075427.
36. Starodub, E.; Bostwick, A.; Moreschini, L.; Nie, S.; El Gabaly, F.; McCarty, K. F.; Rotenberg, E. In-Plane Orientation Effects on the Electronic Structure, Stability, and Raman Scattering of Monolayer Graphene on Ir(111). *Phys. Rev. B* **2011**, *83*, 125428.
37. Pereira, V. M.; Dos Santos, J. M. B. L.; Castro Neto, A. H. Modeling Disorder in Graphene. *Phys. Rev. B* **2008**, *77*, 115109.
38. Lacovig, P.; Pozzo, M.; Alfé, D.; Vilmercati, P.; Baraldi, A.; Lizzit, S. Growth of Dome-Shaped Carbon Nanoislands on Ir(111): The Intermediate between Carbidic Clusters and Quasi-Free-Standing Graphene. *Phys. Rev. Lett.* **2009**, *103*, 166101.
39. Chen, H; Zhu, W.; Zhang, Z. Contrasting Behavior of Carbon Nucleation in the Initial Stages of Graphene Epitaxial Growth on Stepped Metal Surfaces. *Phys. Rev. Lett.* **2010**, *104*, 186101.
40. Cui, Y.; Fu, Q.; Zhang, H.; Bao, X. Formation of Identical-Size Graphene Nanoclusters on Ru(0001). *Chem. Commun.* **2011**, *47*, 1470–1472.